中國機械工程學刊第四十五卷第六期第 585~594 頁(民國一百一十三年)
Journal of the Chinese Society of Mechanical Engineers, Vol.45, No.6, pp585~594 (2024)

Research and Experimentation on Trajectory Optimization for Cotton-Picking Robot Arm

Liao Caiwen*, Hao Jiancheng*, Gulbahar・Tohti**, Orkin・Rahim*** and Mamtimin・Geni****

Keywords：Cotton picking robot; Time optimal trajectory planning; Quintic nonuniform B-spline curve; Particle swarm optimization

ABSTRACT

The cotton-picking robot, a vital tool in modern agriculture, requires meticulous planning of its manipulator's operational path to optimize harvesting costs, quality, and efficiency. Addressing the issues of operational efficiency, vibration, and impact generated during the movement of the mechanical arm for long-staple cotton picking, this study introduces a time-optimal trajectory planning strategy. Analyzing the picking path, this article employ an S-shaped curve for speed control, enabling flexible speed planning methods like four, five, and seven-segment planning. This ensures stable and efficient robot operation across diverse scenarios. Integrating a fifth-order non-uniform B-spline curve with an improved particle swarm algorithm further enhances trajectory planning, significantly reducing interpolation time and improving accuracy. Experimental results show an average interpolation time of 0.24s, with a minimum of 0.232s, representing a nearly twofold reduction compared to traditional methods. This rapid and efficient approach supports autonomous cotton-picking robot operation and serves as a reference for trajectory planning in other agricultural robots.

Paper Received April, 2024. Revised August, 2024. Accepted November, 2024. Author for Correspondence: Gulbahar·Tohti.

* *Graduate Student，School of Mechanical Engineering, Xinjiang University, Urumqi, Xinjiang 830017,China；*

***Assistant Professor，School of Mechanical Engineering, Xinjiang University, Urumqi, Xinjiang 830017,China；*

****Assistant Professor，Tacheng Special Equipment Inspection and Testing Institute, Tacheng, Xinjiang 834700, China；*

**** *Professor，School of Mechanical Engineering, Xinjiang University, Urumqi, Xinjiang 830017，China；and School of Mechanical and Electrical Engineering, Shihezi University, Shihezi, Xinjiang 832003, China.*

INTRODUCTION

The main production areas of long-staple cotton in China are located in Xinjiang, which is renowned for its exceptional quality and serves as a high-quality raw material for high-end textiles and special textiles (Hu Chunle et al.2023). Traditional spindle-type cotton pickers are prone to damaging cotton fibers during the picking process, leading to compromised quality. Therefore, the harvesting of long-staple cotton currently relies heavily on inefficient and costly manual methods, which is a crucial factor restricting the growth and strengthening of China's long-staple cotton industry (BM AZIMOV et al.2023). The development of efficient and precise harvesting robots for long-staple cotton is an important technological approach for implementing the strategy of building a strong cotton-producing country through machine substitution.

The trajectory planning of cotton-picking robots is the key to enhancing harvesting efficiency, which relies heavily on precise recognition and positioning technologies. Currently, due to the diversity and complexity of cotton growth environments, research on cotton-picking manipulator arms at home and abroad is still in its infancy. Existing studies have primarily focused on optimizing picking paths and improving positioning accuracy. For instance, Ma Jianlin optimized cotton-picking paths via simulated annealing & genetic algorithms (Ma Jianlin et al., 2018). Zhang Hao assessed cotton maturity using morphological features & Hough transform, though practical efficacy needs improvement (Zhang Hao et al., 2015). USN Rao proposed a cotton-picking robot based on dynamic Freeman coding (U Rao et al.,2013). Liu Xiangfei achieved trajectory planning for robots under jerk & velocity constraints, using cubic NURBS interpolation (Li Xiangfei et al., 2023). Liu C investigated high-speed Delta robot planning with a 4-3-3-4 polynomial (Liu, C et al.,2020). Lin, C.-J. proposed an enhanced automatic TCP calibration method applied to six-degree-of-freedom collaborative robots, achieving high-precision non-contact calibration, optimizing robotic arm trajectory planning, and enhancing efficiency and accuracy (Line，C-J et al，2023). Wang, C.-C research on trajectory planning of robotic arms based on dynamic double pendulum crank mechanism, utilizing CNN, GPR, and BPNN for enhanced prediction of nonlinear and chaotic motions (Wang, C.-C,et al 2021).

Cao Yuting proposed a time-optimal trajectory planner leveraging B-spline interpolation & linear programming, significantly enhancing operational efficiency (Cao Yuting et al., 2024). Lu S addressed smooth motion for 3-DOF robots using minimum-jerk quintic polynomials (Lu S et al.,2020). Jiayu Wang et al. mitigated planning issues with a 3-5-3 segmented polynomial method for 6-DOF limbs (Jiayu Wang，et al,2024). Baoju Wu et al. optimized paths with quasi-uniform B-splines for efficiency & smoothness (Baoju Wu,et al). Saravnan R improved accuracy & stability with NURBS & fuzzy functions (Saravnan R et al., 2008). Corke optimized joint trajectories via cubic polynomials (Corke eta al., 2017).

However, as cotton-picking robots continue to evolve, new challenges arise for trajectory planning. Based on existing research, this paper proposes a binocular vision-based trajectory planning optimization algorithm that combines S-shaped curve velocity planning with quintic non-uniform rational B-spline curves for trajectory planning. Additionally, an improved particle swarm optimization algorithm is utilized for time-optimal planning. Simultaneously, the D-H modeling method is used to establish a manipulator arm model, providing a theoretical foundation and technical support for the path planning of cotton-picking robots. These studies lay a solid foundation for the further development of cotton-picking robots.

MATERIALS AND METHODS

Agricultural Characteristics of Cotton

Due to various influencing factors such as cotton variety, region, and lighting duration, there exist significant differences in the physical parameters of different cotton bolls from long-staple cotton. In this study, the Xin hai 54 long-staple cotton variety from the Aksu region of Xinjiang was chosen as the experimental material. Sampling was conducted at the end of October with a water content of 9.5% in cotton bolls.

Trajectory Planning Overview

Trajectory planning refers to the curve formed by the continuous change of the position of a moving point in space over time, which is essentially the planning of time by correlating paths with specific time points. For cotton-picking manipulator arms, trajectory planning can be further categorized into two planning methods: joint space planning and Cartesian space planning. The determination of each path point is typically based on the desired posture and position of the tool coordinate system {T} relative to the workstation coordinate system {S}.

In joint space trajectory planning, the joint variables of the manipulator arm are transformed into functions closely related to time. By limiting the angular velocity and angular acceleration, the desired posture and position of each point can be obtained. On the other hand, Cartesian space trajectory planning involves converting the displacement, velocity, and acceleration of the manipulator arm's end-effector in Cartesian space into time-dependent functional expressions, thereby clarifying the spatial path morphology between path points (Chen Zhuang, 2020; Kuang Wenlong et al., 2020).

S-shaped Curve

The S-shaped acceleration and deceleration strategy significantly reduces the impact on the control system by achieving smooth transitions in the velocity curve, making the interpolation process more flexible and compliant. Additionally, the continuous variation of acceleration during acceleration and deceleration introduces a new variable, *j*, known as jerk, which reflects the change in acceleration over time. This innovation not only enriches the toolbox of control engineering but also enhances the stability of system operation.

$$j = \frac{d_a}{d_t} \tag{1}$$

The maximum system speed, $v_{\max}$, reveals its operational limits, while the maximum acceleration, $a_{\max}$, embodies the peak acceleration and deceleration capabilities. On the other hand, jerk (*j*) demonstrates the flexibility and stability characteristics of the system. Greater flexibility leads to larger overshoots and shorter operation times, while lower flexibility results in smaller overshoots and longer operation times. Typically, when calculating the trajectory given the initial and final positions and initial and final speeds $\left(\hat{q}_0, \hat{q}_1, \hat{v}_0, \hat{v}_1, \hat{v}_{\max}, \hat{v}_{\min}, \hat{a}_{\max}, \hat{a}_{\min}, \hat{j}_{\max}, \hat{j}_{\min}\right)$ the necessary transformations are required to facilitate the computation.

Joint Space Trajectory Planning

Joint space trajectory planning involves utilizing models such as polynomials, parabolas, and spline curves for planning the individual joints of a manipulator arm. During the motion of the manipulator arm along the planned trajectory, it is crucial to maintain continuous and smooth changes in the velocity and acceleration of each joint. This ensures the stability of the manipulator arm's joints, minimizes vibrations and impacts on the mechanical system, and extends the lifespan of the manipulator arm（Ma Xiaoxiao,2019）. In this section, we optimize the manipulator arm trajectory based on a fifth-order non-uniform B-spline interpolation and combine it with a particle swarm optimization algorithm to achieve optimal trajectory timing.

$$\begin{cases} q_0 = \sigma\hat{q}_0,\ q_1 = \sigma\hat{q}_1,\ v_0 = \sigma\hat{v}_0,\ v_1 = \sigma\hat{v}_1 \\ v_{max} = \frac{(\sigma+1)}{2}\hat{v}\max + \frac{(\sigma-1)}{2}\hat{v}\min \\ v_{min} = \frac{(\sigma+1)}{2}\hat{v}\min + \frac{(\sigma-1)}{2}\hat{v}\max \\ a_{max} = \frac{(\sigma+1)}{2}\hat{a}\max + \frac{(\sigma-1)}{2}\hat{a}\min \\ am_{in} = \frac{(\sigma+1)}{2}\hat{a}\min + \frac{(\sigma-1)}{2}\hat{a}\max \\ j_{max} = \frac{(\sigma+1)}{2}\hat{j}\max + \frac{(\sigma-1)}{2}\hat{j}\min \\ j_{min} = \frac{(\sigma+1)}{2}\hat{j}\min + \frac{(\sigma-1)}{2}\hat{j}\max \end{cases} \quad (\sigma = sign(\hat{q}_1 - \hat{q}_0)) \qquad (2)$$

Quintic Non-uniform B-spline Trajectory Planning

Utilizing the centroid points obtained from binocular vision as critical path points during the harvesting process of the manipulator arm, a B-spline curve function is employed to transform the junctions of each trajectory segment into smooth curves for fitting and connection. This approach not only ensures the continuity of high-order derivatives in trajectory planning, satisfying the requirements of boundary conditions and derivative continuity, but also exhibits local support, minimizing the change rate of joint displacements. Furthermore, due to its excellent scalability, this method can flexibly cope with complex scenarios involving multiple path points. By applying quintic non-uniform B-spline trajectory planning for the manipulator arm during harvesting, high-precision and high-stability trajectory planning for the manipulator arm is achieved（Wu Junli，2016）.

The fundamental properties of non-uniform rational B-spline curves

The non-uniform rational B-spline curve can be expressed as:

$$C(u) = \frac{\sum_{r=i}^{i+5} d_i R_{i,k}(u) w_i}{\sum_{r=i}^{i+5} R_{i,k}(u) w_i} \qquad (3)$$

In the formula, $d_i (i = 0,1,2,...,n)$ represents the control points corresponding to the B-spline curve, w_i represents the weights associated with all the control points, and $R_{i,k}(u)$ denotes a quintic non-uniform rational B-spline basis function, which is constructed based on non-periodic and non-uniform knots U.

$$U = \left\{ \underbrace{a,...,a}_{k+1},...,u_{k+1},...,u_{m-k-1},\underbrace{b,...,b}_{k+1} \right\} \qquad (4)$$

In the above formula, k represents the degree of the non-uniform rational B-spline curve, and in this paper, k=5. The variable i indicates the index of the knots in the non-uniform rational B-spline curve. The r-th derivative of any point on the B-spline curve, denoted as $C^r(u)$, can be obtained as follows:

$$C^r(u) = \sum_{j=i-k+r}^{i} d_j^r N_{j,k-r}(u) \qquad u_i \le u \le u_{i+1}$$

$$d_j^l = \begin{cases} d_j & l = 0 \\ (k+1-r)\dfrac{d_j^{l-1} - d_{j-1}^{l-1}}{u_{j+k+1-l} - u_j} & l = 1,2,...,r \\ & j = i-k+l,...,i \end{cases} \qquad (5)$$

Constructing a Joint Space Interpolation Function

The main process of B-spline interpolation comprises two key steps:

a. When the time nodes are not normalized, they undergo parameterization to derive node parameter values u1 that correspond to the data points p_i.

b. Building on the previous step, $n+k$ equations are formulated based on the motion information of the start and end points to determine the new control vertices d_i.

Through these steps, a B-spline curve can be constructed that interpolates the given data points while satisfying the motion constraints at the start and end points. This curve provides a smooth and continuous representation of the data, suitable for applications in robotics, animation, computer-aided design, and other fields.

Improved Particle Swarm Optimization Algorithm

Due to the employment of a fixed inertia coefficient ω, the particle swarm optimization (PSO) algorithm often tends to become trapped in local optima, thus failing to locate the global optimal solution （Jiang Guoquan et al., 2017）.Consequently, dynamically adjusting the inertia coefficient can effectively address this issue.

$$\omega = \begin{cases} \omega_{min} - \dfrac{(\omega_{max} - \omega_{min}) \times (f_i - f_{min})}{f_{avg} - f_{min}} \\ \omega_{max} f_i > f_{avg} \end{cases} \qquad (6)$$

Here, ω_{max} and ω_{min} represent the maximum and minimum inertia coefficients, respectively. The current fitness value of particle i is denoted as f_i, the average fitness value of all particles is represented by f_{avg}, and the minimum fitness value among all particles is indicated by f_{min}. These parameters collectively influence the performance and outcome of the algorithm. To achieve the desired output during the optimization process, it is crucial to carefully select appropriate acceleration constants, as shown in equations 7 and 8.

$$c_1 = c_{1,int} + \frac{c_{1,fin} - c_{1,int}}{t_{max}} \times t \qquad (7)$$

$$c_2 = c_{2,int} + \frac{c_{2,fin} - c_{2,int}}{t_{max}} \times t \qquad (8)$$

In the given formula, t represents the runtime duration of the algorithm. The best position of the particles is calculated according to formula (9) to obtain accurate results (Li Zhi et al., 2004).

$$\hat{Y} = \arg\min_Y tr(Y^T(D-Y))Y.(Y^T DY)^{-1} \quad (9)$$

Based on the preset conditions of path length, velocity, acceleration, and harvesting time during the cotton picking process of the mechanical arm, the six joints of the mechanical arm must satisfy certain motion constraint equations (10-13). The kinematic constraints for time-optimal trajectory planning in joint space are as follows:

$$\dot{p}_0 = v_0 \quad (10)$$

$$\dot{p}_f = v_f \quad (11)$$

$$\ddot{p}_0 = a_0 \quad (12)$$

$$\ddot{p}_f = a_f \quad (13)$$

$$\begin{cases} \left| \sum_{j=i-f}^{i} d_j^1 N_{k-1,j}(t_i) \right| \le V_{\max} \\ \left| \sum_{j=i-f}^{i} d_j^2 N_{k-2,j}(t_i) \right| \le A_{\max} \; i = 6,7,...,n+4 \\ \left| \sum_{j=i-f}^{i} d_j^3 N_{k-3,j}(t_i) \right| \le V_{\max} \end{cases} \quad (14)$$

The model for the time-optimal trajectory planning problem in joint space, under the satisfaction of motion constraints, is formulated as:

$$\text{s.t.} \begin{cases} g_1(t_i) - V_{\max} \le 0 \\ g_2(t_i) - A_{\max} \le 0 \quad i = 1,2,...,n+4 \\ g_3(t_i) - J_{\max} \le 0 \end{cases} \quad (15)$$

This optimization problem involves nonlinear constraints, and the structure of function $g_r(t_i)$ is complex, requiring a solution that integrates various constraints. To address this issue, a novel objective function is constructed by combining the exterior point function method with the basic particle swarm optimization algorithm.

Based on the characteristics of non-uniform B-spline curves and the behavior of the manipulator during operation, this paper sets the control points of the velocity, acceleration, and jerk curves for each joint as the limiting values of the constraint conditions. The control points can be selected as max{0, g ' (t)} to penalize points that violate the constraints. Subsequently, the particle swarm optimization algorithm is employed to find the new optimal solution for the objective function.

$$F(t) = f(t) + \max\{0, g,(t)\}, (r = 1,2,3) \quad (16)$$

Time-Optimal Trajectory Planning Based on an Improved Particle Swarm Optimization Algorithm

Optimization Criteria

a. The time performance index is defined as the time interval between every two path points, represented as $t_{(i+1)}-t_i$. The time-optimal model is constructed as follows:

$$Y_1 = \sum_{i=1}^{n-1}(t_{(i+1)} - t_i) = t_n \quad (17)$$

In the formula, Y_1 represents the total time of the manipulator's picking process, where i denotes the path point, and Y_1 is used to evaluate the work efficiency of the manipulator's picking process.

b. Jerk Performance Index

$$Y_2 = \sum_{j=1}^{N} \sqrt{\frac{1}{T}\int_0^T \left(jerkj(t)\right)^2 dt} \quad (18)$$

In the formula, Y_2 represents the average acceleration to be optimized for each joint of the manipulator, where j denotes the joint index and N is the number of joints. In this paper, a six-degree-of-freedom manipulator is employed, with N=6. *jerkj(t)* is the jerk curve function of the jth joint, which can evaluate the stability of the manipulator's picking process (Gao Xiaopeng,et al., 2023).

Spatial Positioning of Cotton

During the cotton picking process, the picking robot needs to accurately locate the cotton target object in outdoor environments with strong light and other complexities (Liu Yafang et al., 2022). To this end, an efficient and precise binocular matching method is adopted in this paper (Zhang Guohui et al., 2024). This method relies on a deep learning model to accurately capture the location and shape information of cotton, and achieves rapid matching through an innovative matching equation. After the matching is completed, the calculated disparity distance is used for precise ranging, which further enables spatial positioning.

A binocular camera platform, constructed with 5-megapixel industrial cameras from RealView, is presented. Table 1 provides a detailed enumeration of the cameras' technical specifications. Figure 1 offers a visual illustration of the binocular camera's exterior design. As depicted in Figure 2, the coordinate system is bifurcated into a world coordinate system (x, y, z), with the camera center as the origin, and an image coordinate system (u, v), anchored at the vertex of the image plane. This dual-system approach ensures a clear representation of cotton's position in both the real-world space and the image domain. By leveraging a tailored positioning equation (20), precise spatial localization of cotton target objects is achieved, facilitating advanced automation in mechanical engineering applications.

$$\begin{cases} x = (x_i - x_0) \times z / f \\ y = (y_i - y_0) \times z / f \\ z = f \times b/d \end{cases} \quad (19)$$

In mechanical engineering applications, x, y, z (mm) represent the 3D coordinates of cotton in the world coordinate system, while x_i, y_i (mm) denote their 2D projections in the image coordinate system. The camera center's 2D coordinates in the image plane are x_0, y_0 (mm). The baseline b (mm) and focal length f

(mm) of the camera system characterize the geometric setup. The disparity d (mm), derived from image analysis, encodes depth information. This mathematical framework underpins precision measurement and control in vision-guided mechanical engineering systems, enabling accurate localization and inspection of cotton or similar materials.

Table 1 Technical parameters of binocular camera

Hardware performance		Calibration parameters	
output format	MJPEG/YUV	focal distance(left)	2043.875
frame rate	30FPS	focal distance(right)	2064.712
maximum resolution	2592*1944	image center(left)	1151.527* 925.810
baseline	5cm	image center(right)	1280.002* 960.588

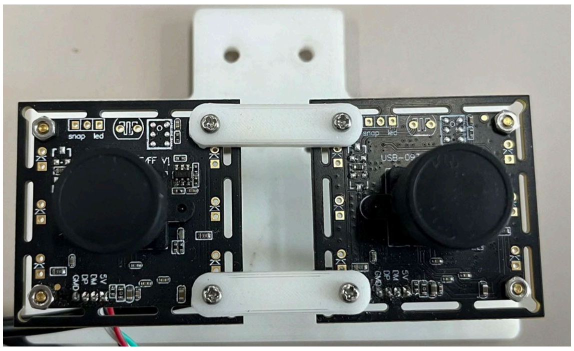

Fig 1 Physical image of binocular camera

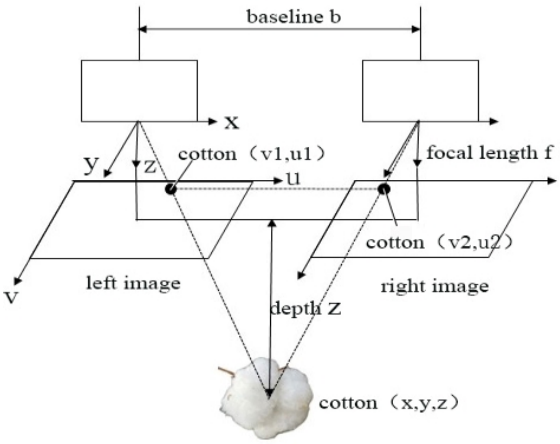

Fig 2 Schematic diagram of binocular camera coordinate System

EXPERIMENTS AND VERIFICATION

Binocular Vision Positioning Experiments

As depicted in Figure 3, the first-generation cotton-picking robot developed by the team utilizes a binocular vision system to precisely acquire the position information of cotton bolls. The controller processes the data obtained by the binocular cameras, computing the optimal trajectory for the cotton-picking manipulator. Upon precise positioning above the cotton, a negative pressure fan is activated, generating strong suction through the cotton-sucking hose to effortlessly pluck and transport the cotton into a storage bin.

Prior to harvesting, binocular calibration and hand-eye calibration are performed to ascertain camera intrinsic and extrinsic parameters along with transformation matrices for image rectification. The captured images undergo cotton segmentation and matching, facilitating the calculation of 3D coordinates of picking points, thereby providing data support for precise harvesting. Figure 4 illustrates the cotton field experimentation of this first-generation cotton-picking robot, demonstrating its ability to accurately detect cotton positions and accomplish picking tasks. Table 2 presents the data of 15 cotton bolls with similar growth heights, which were acquired through visual localization.

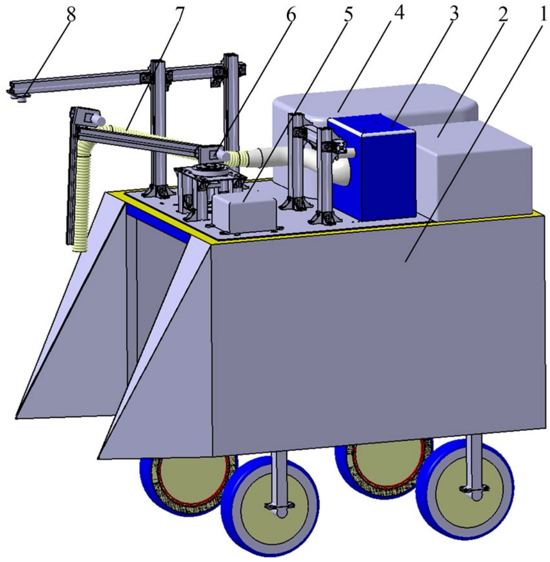

1.chassis,2.battery box, 3. negative pressure fan, 4.cotton storage box,5.controller;,6.robotic arm,7.cotton suction hose,8.binocular camera

Fig 3 First-generation prototype of cotton-picking robot

（a）Cotton Identification （b） Path Planning （c）Suction Harvestin

Fig. 4 Cotton binocular vision positioning experiment scene

Table 2 binocular vision cotton positioning results

Number	X/mm	Y/mm	Z/mm
1	51.121	168.334	701
2	84.842	147.494	734
3	80.062	107.575	751
4	58.217	82.333	721
5	111.272	68.883	736
6	173.951	76.114	741
7	99.110	149.229	720
8	120.919	106.751	724
9	192.965	160.769	746
10	162.154	114.928	695
11	239.766	133.209	710
12	188.772	114.137	693
13	384.114	104.148	713
14	229.306	58.464	718
15	191.459	50.099	725

Trajectory Planning Simulation Testing

During cotton harvesting, the position and orientation of cotton bolls rotate relative to the stationary cotton-picking robot. The robotic arm undertakes trajectory planning for cotton at similar heights, enabling stratified picking. Assuming a field operation speed of 119 cm/s, this is designated as the maximum joint velocity (v_{max} = 119 cm/s). Maximum acceleration (a_{max} = 500 cm/s^2) and jerk (j_{max} = 500 cm/s^3) are specified for the arm during harvesting. Figure 5 showcases the initial shortest path obtained via simulated annealing. Subsequently, the feasibility of attaining maximum velocity or acceleration is evaluated based on path length and harvesting time, with S-curve velocity profiles applied to each segment. Table 3 outlines the DH parameters of the robotic arm.

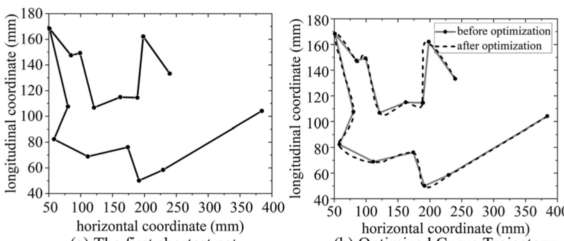

(a) The first shortest pat (b) Optimized Curve Trajectory

Fig 5 Track planning results

Table 3 D-H matrix of each joint of the manipulator

Connecting Rod i	θ_i（rad）	d	α_i(rad)	α_i
1	-170°～170°	0	0	0
2	-90°～165°	420	-π/2	155
3	-205°～270°	0	0	650
4	-270°～270°	0	-π/2	140
5	-160°～95°	920	π/2	0
6	-400°～400°	0	-π/2	60

As depicted in Figure 6, velocity profiling results for harvesting paths reveal that the maximum velocities of the 1st and 15th segments are below the prescribed maximum robot motion speed. Under the given constraints, a five-segment S-curve velocity profile is adopted for these paths, eliminating uniform acceleration and deceleration phases. For segments 2 to 14, where picking points are closely spaced, a four-segment S-curve is planned, omitting uniform acceleration, deceleration, and constant velocity stages. Furthermore, utilizing the modified Particle Swarm Optimization (PSO) algorithm proposed herein, with 500 iterations, inertia weights w_{max}=0.5 and w_{min}=0.3, cognitive constants C_{1f}=0.05 and C_{1i}=0.02, and social constants C_{2f}=0.05 and C_{2i}=0.02, a swarm size of 50 particles is selected.

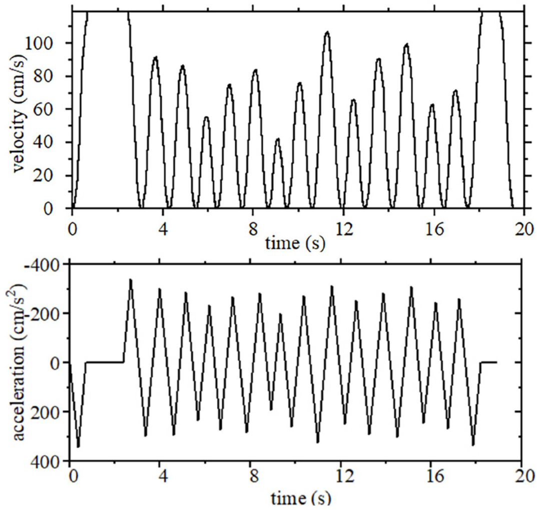

Fig. 6 Path speed planning of each section

As shown in Figure 7, the fifth-order polynomial interpolation method was employed for trajectory planning at the picking points, and combined with the optimized particle swarm optimization algorithm, the angular velocity, angular acceleration, and angular jerk variation charts for each joint of the robotic arm were obtained. However, upon analyzing these charts, it was observed that while the velocity curves were continuous, the acceleration and jerk curves exhibited discontinuity. Specifically, at t=5s, there was a sudden change in the acceleration of each joint, and during the picking process, there were significant variations in the joint velocity and acceleration. For instance, within the first 1 second of activation, the acceleration of joint 1 and joint 2 rapidly increased from 0 rad/s^2 to 9.346 rad/s^2 and 10.103 rad/s^2, respectively, with similar trends observed in other joints. This short-term acceleration caused an impact on the mechanical system, potentially affecting the smooth progress of the picking work.

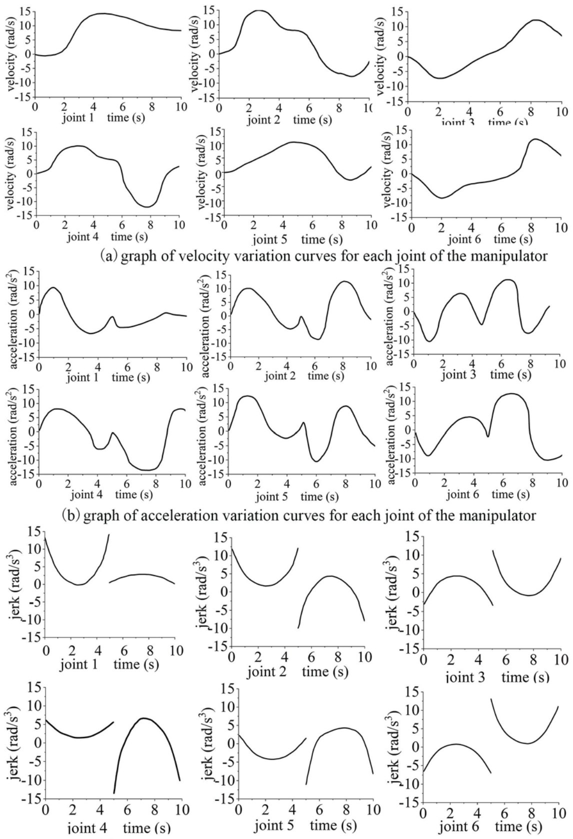

(a) graph of velocity variation curves for each joint of the manipulator

(b) graph of acceleration variation curves for each joint of the manipulator

(c) Graph of jerk variation curves for each joint of the robotic arm

Fig.7 Joint characteristic diagram for time-optimal trajectory planning using quintic polynomial

During simultaneous motions of robotic arm joints, a joint's velocity can abruptly decrease from its maximum to minimum (or vice versa) within a short period, resulting in velocity spikes. To mitigate the likelihood of such velocity spikes and enhance the smoothness and efficiency of the robotic arm's movements, this paper employed fifth-order non-uniform B-spline curve interpolation combined with an improved particle swarm optimization algorithm. As depicted in Figure 8, a comparison of the angular, angular velocity, and angular acceleration profiles at the end effector and individual joints of the robotic arm before and after the optimization reveals significant improvements. Specifically, the velocity range at the end effector was reduced from -9.392 rad/s to 9.089 rad/s to -9.287 rad/s to 6.614 rad/s, and the acceleration range was narrowed from -28.239 rad/s² to 31.210 rad/s² to -17.557 rad/s² to 12.706 rad/s². Additionally, for each joint, the optimized angular velocity range decreased from -0.019 rad/s to 0.030 rad/s to -0.015 rad/s to 0.020 rad/s, and the angular acceleration range decreased from -0.069 rad/s² to 0.072 rad/s² to -0.046 rad/s².

As demonstrated in Figure 9, the optimized robotic arm exhibited reduced joint speeds and mitigated sudden changes during startup, effectively alleviating impact issues. Through iterative optimization using the particle swarm algorithm, the interpolation time using fifth-order non-uniform B-spline curve interpolation was reduced by half compared to fifth-order polynomial interpolation. The average interpolation time decreased from 0.52s to 0.24s, and the shortest interpolation time was reduced from 0.516s to 0.232s. This significantly improved the efficiency and stability of trajectory planning, contributing to enhanced accuracy and efficiency in harvesting operations.

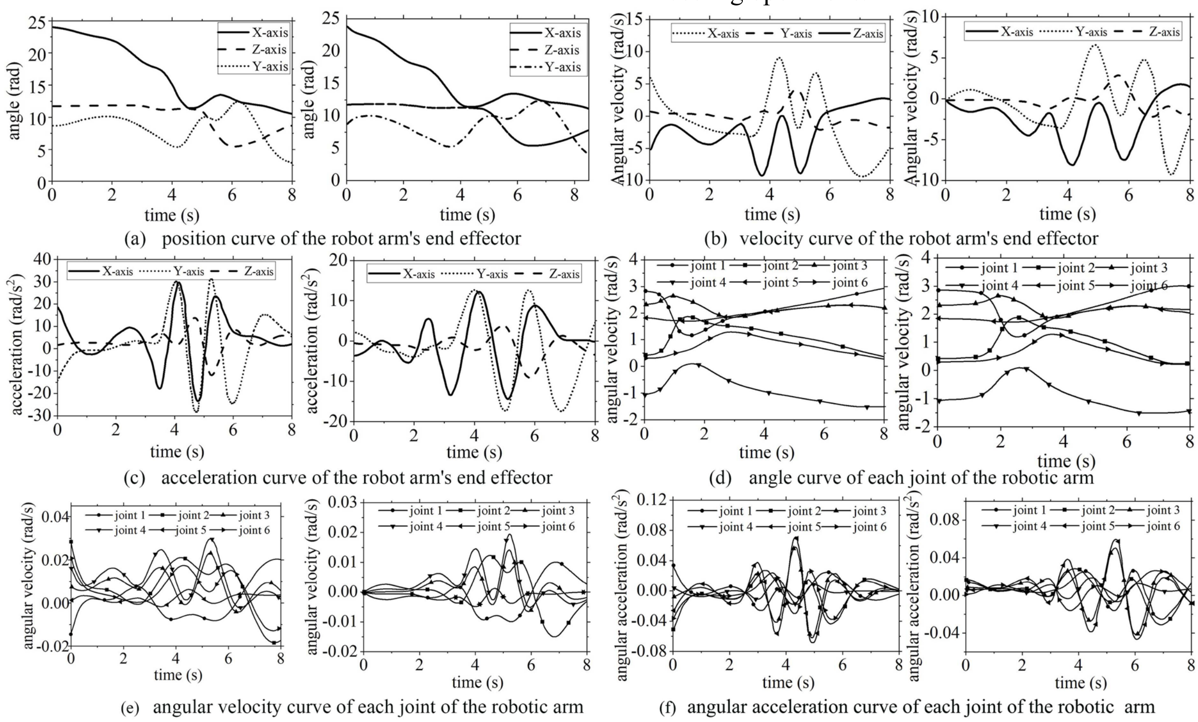

(a) position curve of the robot arm's end effector

(b) velocity curve of the robot arm's end effector

(c) acceleration curve of the robot arm's end effector

(d) angle curve of each joint of the robotic arm

(e) angular velocity curve of each joint of the robotic arm

(f) angular acceleration curve of each joint of the robotic arm

Fig. 8 Time optimal trajectory planning using non-uniform quintic B-spline curve

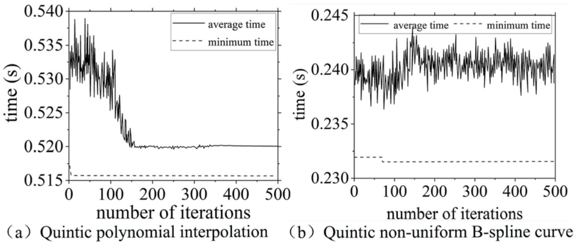

Fig. 9 Time optimal particle adaptation curve

Experimental Verification and Analysis

To accurately evaluate the performance of the trajectory planning model, validation experiments were conducted within a laboratory setting. Firstly, based on the previously acquired coordinates of fifteen cotton bolls, the bolls were arranged in an open area of the laboratory, ensuring that all bolls were positioned at similar heights to minimize the influence of external factors on the experimental results.

Subsequently, both the pre-improvement and post-improvement algorithms were programmed into the robotic arm controller. In order to quantify and assess the performance of these two models, the trajectory planning time for the robotic arm to move from the first picking point, sequentially through thirteen cotton picking points, and finally reach the last picking point was recorded. Multiple trials were conducted, and during the data analysis phase, outliers and data with significant errors were excluded to obtain more accurate and reliable average trajectory planning time data. As shown in Table 4, the average trajectory planning time data under different control models are presented.

Table 4 The average trajectory planning time under different control models

Model	Average Trajectory Planning Time/s
before improvement	40.3
after improvement	34.5

Based on the data presented in Table 3, a substantial difference in trajectory planning time can be observed between the pre-improvement and post-improvement models. The improved model, with its reduced average trajectory planning time, not only accelerates the computation of optimal paths but also enhances the overall efficiency of trajectory planning. Furthermore, this model exhibits reduced velocity fluctuations during operation, thereby strengthening operational smoothness and enhancing the reliability of the entire system.

CONCLUSION

This paper addresses the issues of execution efficiency, vibration, and impact during the operation of a long-staple cotton harvesting robotic arm. To tackle these problems, a time-optimal trajectory planning approach is proposed. The main conclusions are as follows:

(1) The trajectory of the robotic arm is planned using fifth-order non-uniform B-spline curve interpolation combined with an improved particle swarm optimization algorithm. Compared to the pre-improvement state, the range of velocity variations at the end effector of the optimized robotic arm is reduced from -9.392 rad/s to 9.089 rad/s to -9.287 rad/s to 6.614 rad/s, and the acceleration range is narrowed from -28.239 rad/s² to 31.210 rad/s² to -17.557 rad/s² to 12.706 rad/s². Additionally, for each joint, the post-processed angular velocity range decreases from -0.019 rad/s to 0.030 rad/s to -0.015 rad/s to 0.020 rad/s, and the angular acceleration range is reduced from -0.069 rad/s² to 0.072 rad/s² to -0.046 rad/s² to 0.060 rad/s². These improvements effectively reduce the velocity spikes during simultaneous joint motions of the robotic arm.

(2) The use of fifth-order polynomial interpolation combined with a particle swarm optimization algorithm for trajectory planning of the cotton-picking robotic arm results in discontinuous acceleration and jerk, causing impacts on the mechanical system and affecting efficiency. Theaverage interpolation time for this method is 0.52s, with a minimum of 0.516s. In contrast, the adoption of S-curve control for harvesting speed, in conjunction with fifth-order non-uniform B-spline curve interpolation and the improved particle swarm optimization algorithm, significantly shortens the interpolation time to an average of 0.24s, with a minimum of 0.232s, thereby enhancing harvesting efficiency and providing a rapid and effective solution for path planning.

(3) The improved model achieves a reduction in trajectory planning time from 40.3 seconds to 34.5 seconds, enhancing planning efficiency. Simultaneously, the model exhibits improved speed and accuracy in calculating optimal paths, minimizes velocity spikes during operation, and enhances operational smoothness and reliability.

ACKNOWLEDGEMENTS

This project was supported by the National Natural Science Foundation of China, Regional Science Foundation Project (Grant No. 12162031), the Major Science and Technology Special Project of Xinjiang Uyghur Autonomous Region (Grant No. 2022A02010), and the "Tianshan Talents" Cultivation Plan of Xinjiang Uyghur Autonomous Region (Grant No. 2022TSYCJC0055).

The authors would wish to sincerely thank the students, laboratory staf, and mentors for their valuable contributions in the entire process of the research work.

REFERENCES

Baoju Wu, Xiaohui Wu, Nanmu Hui, et al. Trajectory Planning and Singularity Avoidance Algorithm for Robotic Arm Obstacle Avoidance Based on an Improved Fast Marching Tree[J]. Applied Sciences, 2024, 14(8). https://doi.org/ 10.3390/ APP14083241

B M AZIMOV, N N OMONOV, J SH NORQULOV, et al. Mathematical modeling and optimal motion control of horizontal spindle apparatuses of cotton pickers[J]. IOP Conference Series: Earth and Environmental Science,2023,1231(1). https://doi.org/10.1088/1755-1315/1231/1/012058.

Cao Yuting, Wang Jintao, Liu Mingmin, et al. A Time-Optimal Synchronized Trajectory Planning Method for Robot Pose [J]. Modular Machine Tool & Automatic Manufacturing Technique, 2024(2): 61-65. https://doi.org/10.13462/j.cnki.mmtamt.2024.02.013.

Chen Zhuang. Research on robot recognition, positioning and trajectory planning based on binocular vision [D]. Qingdao University of science and technology, 2020.

Corke P .Robotics, Vision and Control[J].Springer Tracts in Advanced Robotics, 2017, 118. https:// doi.org/0.1007/ 978-3-319-54413-7.

Field G , Stepanenko Y .Iterative dynamic programming: an approach to minimum energy trajectory planning for robotic manipulators[C]//Robotics and Automation, 1996. Proceedings. 1996 IEEE International Conference on. IEEE, 1996. https://doi.org/ 0.1109/ ROBOT.1996.506579.

Gao Xiaopeng, Liu Dongyu, Huo Cong. A Review of Motion Planning Research for Unmanned Surface Vessels [J]. Ship Science and Technology, 2023, 45(16): 1-6. https://doi.org/10.3404/j.issn.1672-7649.2023.16.001.

Hu Chunlei, Li Xiaohua, Wang Ruixia, et al. Report on the Industrial Development of the Cotton Processing Industry in 2022 (Part 2) [J]. China Cotton Processing, 2023 (02): 4-16. https://doi.org/10.3969/j.issn.1003-0662.2023.01.002.

Jiang Guoquan, Yang Xiaoya, Wang Zhiheng, et al. Crop row detection in wheat field based on image feature point particle swarm clustering algorithm [J]. Journal of agricultural engineering, 2017,33 (11): 165-170. https://doi.org/ CNKI:SUN:NYGU.0.2017-11-021.

Jiayu Wang, Ruyue Sun, Yukun Zheng, et al. White Shark Optimizer Based Time-optimal Trajectory Planning for Supernumerary Robotic Limbs[J]. Engineering Letters, 2024, 32(7):1448-1464.

Kuang Wenlong, Shen Wenlong, Ji Changying, et al. Trajectory tracking control system design and test of agricultural tracked robot [J]. Journal of Northeast Agricultural University, 2020,51 (04): 78-87. https://doi.org/ CNKI:SUN: DB DN.0.2020-04-010.

Liu Xiangfei, Zhao Huan, He Xianming, et al. A novel cartesian trajectory planning method by using triple NURBS curves for industrial robots[J]. Robotics and Computer-Integrated Manufacturing, 2023, https:// doi.org/ 10.1016/ j. rcim.2023.102576.

LIU, C., CAO, GH., QU, YY. et al. An improved PSO algorithm for time-optimal trajectory planning of Delta robot in intelligent packaging. Int J Adv Manuf Technol **107**, 1091–1099 (2020). https://doi.org/10. 1007/ s00170-019-04421-7.

Lin, C.-J.; Wang, H.-C.; Wang, C.-C. Automatic Calibration of Tool Center Point for Six Degree of Freedom Robot. Actuators **2023**, 12, 107. https://doi.org/10.33 90 /act12030107

Li Zhi, Zheng Xiao. Application of particle swarm optimization algorithm in agricultural engineering optimization design [J]. Journal of agricultural engineering, 2004 (3): 15-18. https://doi.org/10. 3901/JME.2008.12.226.

Liu Yafang, Mamtimin • Geni, Gulbahar • Tohti, et al. An Improved SM Spectral Clustering Algorithm for Accurate Cotton Segmentation in Cotton Fields[J]. Journal of Agricultural Mechanization Research, 2022, 44(12):35-41. https://doi.org/ 10.3969/j.issn.1003-188X. 2022.12.006.

Lu S, Ding B, Li Y. Minimum-jerk trajectory planning pertaining to a translational 3-degree-of-freedom parallel manipulator through piecewise quintic polynomials interpolation. Advances in Mechanical Engineering. 2020;12(3). https:// doi.org/10.1177/ 1687814020913667

Ma Jianlin. Research on path planning of cotton picking head of new intelligent cotton picking robot [D]. Chongqing University, 2018.

Ma Xiaoxiao. Welding trajectory planning of welding robot and establishment of simulation platform [D]. Henan University of technology, 2019.

Saravanan R , Ramabalan S , Balamurugan C .Multiobjective trajectory planner for industrial robots with payload constraints[J].Robotica,2008,26(06):753-765. https:// doi.org/ S0263574708004359.

U Rao. Design of automatic cotton picking robot with Machine vision using Image Processing algorithms[J].2013 International Conference on Control, Automation, Robotics and Embedded Systems (CARE), 2013, pp. 1-5.

Wang, C.-C.; Zhu, Y.-Q. Identification and Machine Learning Prediction of Nonlinear Behavior in a Robotic ArmSystem. *Symmetry* 2021,*13*, 1445. https:// doi.org/ 10.3390/sym13081445.

Wu Junli. Research on grasping design and trajectory control of handling manipulator [D]. Yanshan University, 2016. shttps://doi.org/10.7666/d.D01112106

Yang Jintao, Jiang Wengang, Lin Yongcai. Impact optimal trajectory planning algorithm for industrial robots [J]. Science, technology and engineering, 2014, 14 (28): 64-69. https://doi.org/10.3969/j.issn.1671-1815.2014.28. 013.

Zhang Hao. Research on cotton image segmentation and cotton field visual navigation based on machine vision [D]. Xinjiang Agricultural University, 2015. https:// doi.org/ 10.7666/d.Y2887172.

Zhang Guohui, Gulbahar・Tohti, Chen Ping, et al. SFEMM: A cotton binocular matching method based on YOLOv7x[J]. Mathematical Biosciences and Engineering, 2024, 21(3): 3618-3630.https://doi.org/10.3934/mbe.202415.

採棉機器人機械臂軌蹟優化的研究與試驗

廖才文 郝建成 古麗巴哈爾·託乎提
新疆大學機械工程學院

吾爾科木·冉合木
新疆塔城地區市場監管局特種設備檢驗檢測所

買買提明·艾尼
新疆大學機械工程學院和石河子大學機械電氣工程學院

摘 要

在現代農業中採棉機器人發揮著舉足輕重的作用。為實現採摘成本的降低、品質的提升和傚率的提高，其操作路徑需進行精心規劃。本研究針對長絨棉採摘機械臂的執行效率以及在運動過程中所產生振動與衝擊問題，提出瞭一種時間最優軌跡規劃策畧。通過對採摘路徑的深入分析，本文采用 S 型曲線進行速度控制，實現瞭四段、五段和七段等多種靈活的速度規劃方瀀，從而確保機器人在不同場景下都能穩定、高傚地運行。此外，通過將五階非均勻 B 樣條曲線與改進的粒子群算瀀相結合，進一步提升瞭軌跡規劃的精度，顯著縮短瞭插值時間。實驗結果表明，該方瀀的平均插值時間為 0.24 秒，最短插值時間達到 0.232 秒，與傳統方瀀相比，插值時間幾乎減少瞭一半。這種快速高傚的策畧不僅支持棉花采摘機器人的自主運行，而且為其他農業機器人的軌跡規劃提供瞭有益的參考。